Direct Writing of High Frequency Surface Acoustic Wave Devices on Epitaxial $Pb(Zr_{0.20}Ti_{0.80})O_3$ Thin Layers using Focus Ion Beam Etching

R. Salut, W. Daniau, S. Ballandras
Institut FEMTO-ST, UMR 6174 CNRS, Dépt. LPMO,
32 Ave. de l'Observatoire, 25044 Besançon Cedex, France
sylvain.ballandras@femto-st.fr

S. Gariglio, G. Triscone, J.-M. Triscone
DPMC, University of Geneva, 24 Quai E. Ansermet, 1211 Geneva 4, Ecole d'Ingénieurs de Genève (EIG / HES-SO) 4, rue de la Prairie, 1202 Geneva, Switzerland

***Abstract*—We propose an original alternative to lithographic techniques based on the Focused Ion Beam etching technique to fabricate SAW devices by directly "writing" the electrode pattern in the metal overlay. We also explore the RF capabilities of epitaxial $Pb(Zr_{0.20}Ti_{0.80})O_3$ (PZT) thin films deposited onto $SrTiO_3$ single crystal substrates. We found that guided waves can be efficiently excited and detected at frequencies ranging from 3 to 5 GHz. Theory/experiment assessment shows a good predictability of the wave characteristics.**

I. INTRODUCTION

The standard fabrication of surface acoustic wave (SAW) devices exploiting inter-digital transducers (IDTs) on single crystal substrates is based on metal deposition and patterning using photolithography [1]. Such an approach is well suited for large wafer processes and on-trench manufacturing, but poorly adapted to innovative materials generally built on small parts preventing the use of contact lithography or incompatible with stepper-based product lines. On the other hand, these processes are used close to the limits of their capabilities [2] and do not allow for investigating the actual limits of surface acoustic waves and elastic wave guides based on IDTs.

In this work, we investigate the possibility to fabricate IDT directly in one process step, by using focused ion beam (FIB) etching techniques on an epitaxial $Pb(Zr_{0.20}Ti_{0.80})O_3$ (PZT) layer deposited on a $SrTiO_3$ single crystal substrate [3]. For that purpose, we have used our FIB machine (Orsay Physics). A very energetic focused Gallium beam capable to etch almost any material with a resolution smaller than 100 nm is used to directly etch the aluminium layer deposited atop the PZT film. The desired pattern is simply computed and stored as a binary file driving the FIB (this technique does not require any mask as for E-Beam writing techniques). The sample on which the SAW device is fabricated can in principle exhibit any shape and very small surfaces can be processed. The etching duration is typically less than one hour, depending on the exact transducer dimensions. Test devices have been fabricated on PZT epitaxial layers of thicknesses ranging from 100 to 200 nm, allowing for the excitation of 1 micron wavelength Rayleigh-like waves. The test device corresponds to a single-port resonator operating at frequencies ranging from 3 to 5 GHz, depending on the mode order. Coupling factors varying from 0.5 to 1.6 % for the first mode and from 0.8% to 2.8% for the second mode have been measured with Q factors in the in the range of 30-90. This is very promising figures according to the literature and the device configuration that is far from the optimal one (small number of IDT finger pairs together with very short mirrors).

We first briefly recall the basic principle of the FIB etching technique, then we present our test devices and their experimental characterization. We also report on theory experiment assessment, using our periodic finite element/boundary element simulation code. As a conclusion, the actual limit of the technology is discussed.

II. FIB ETCHING TECHNIQUES

The principle of our Focused Ion Beam (FIB) workstation appears very close to the one of a SEM. It is briefly recalled here is has already been detailed in previous work [4]. A probe is fixed on a multi-axis tilt stage located in a high-vacuum chamber to which the ion column is connected. Inside the column, ions are generated, accelerated and focused. The liquid metal ion source provide the accelerated material (in our case gallium). The ions are extracted from the metal surface by applying an electrical field. A liquid metal ion source is extremely intense and its emission area is quite small (~10 nm). The ion column contains all the elements required for the acceleration, focusing and deflection of the ion beam (see fig.1). The ions are accelerated to an energy of 30 keV and electrostatically focused to a beam diameter of a couple of nm. Ion densities are within the 3-10A/cm² range.

The scanning of the ion beam over the sample surface is digitally driven. When the ions hit the sample surface, ions can be implanted, defects generated and sample material

This work has been achieved in the Dominos project framework, funded by the European Community as the InterReg project DOMINOS

removed (due to the large mass of Ga ions). This sputtering allows for local removal of material by means of focused ion beams in a direct writing mode, the one we expect to use for our application.

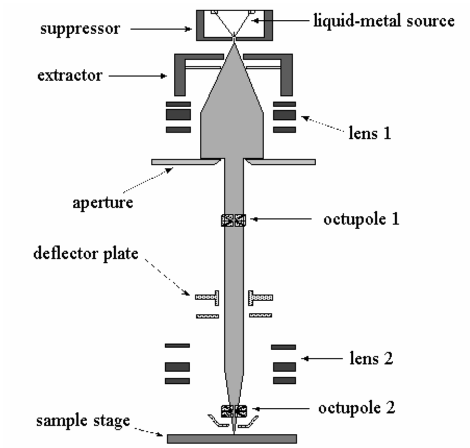

Figure 1. Principle scheme of a FIB column [4].

Our FIB is a double beam device developed by Orsay Physics. This apparatus is built on a scanning electron microscope (SEM) LEO Stereoscan 440 using an eucentric stage (no lateral displacement generated when rotating the stage). It exhibits a 50-to-60°-tilted focused ion beam column compared to the electronic (SEM) column, which guarantees that the sample is tilted faced to the ion beam. The etching rate is typically 0.1 $\mu m^3.nA^{-1}.s^{-1}$. The total etching area is limited to 300×300 µm².

III. SAW DEVICES ON EPITAXIAL $Pb(Zr_{0.20}Ti_{0.80})O_3/SrTiO_3$ SUBSTRATES

A. Epitaxial PZT layers

High quality c-axis $Pb(Zr_{0.2}Ti_{0.8})O_3$ films have been grown on insulating (001) $SrTiO_3$ single crystal substrates by off-axis magnetron sputtering in a 180 mTorr pressure oxygen/argon mixture at a substrate temperature of 510°C [3]. X-ray diffraction analyses confirm the c-axis orientation and the high crystalline quality. The films exhibit finite size effects around the (001) reflection peaks, allowing the measurement of the thickness (150 nm and 200 nm in this case) and showing a high degree of coherence through the entire film. Rocking curves around (001) PZT peaks have a full width at half maximum of 0.025°, a value that corresponds to the dispersion observed on the (001) peak of the single crystal$SrTiO_3$ substrate. Atomic force microscopy topographies reveal flat surfaces with a RMS roughness of 1.2 nm over μ^2 areas. The main limit to the exploitation of such thin films is the actual size of the area for which well controlled film thickness is achievable, i.e. 5×5mm² typically. This imposes to use a technology capable to manufacture test devices on such small substrate to assess their RF SAW properties. This is one of the strongest motivation of the technological development reported in the next section.

B. FIB etching of SAW test devices

In this section, we report on the fabrication and characterization of single-port SAW resonators built using the above-detailed technique. It must be first mentioned that due to the short fabrication range and the manufacturing delay, only small devices were achieved. The first device consisted in a 10-finger-pairs transducer with two 20-strip mirrors, with a strip and gap widths arbitrarily fixed to 250 nm yielding a 1 µm wavelength with an electrode height of 50 nm well suited for the etching process. The acoustic aperture was 40 µm (i.e. 40 acoustic wavelength λ_{ac}) and the length of the device was 30µm. Figures 2 and 3 respectively give a wide view and details of the device, illustrating the accuracy of the pattern. A contact pad also has been manufactured to allow for an easy probing of the device. Furthermore, all the surrounding metal is grounded when probing, providing a good electrical isolation of the device (but possibly generating some unevaluated parasitic capacitance).

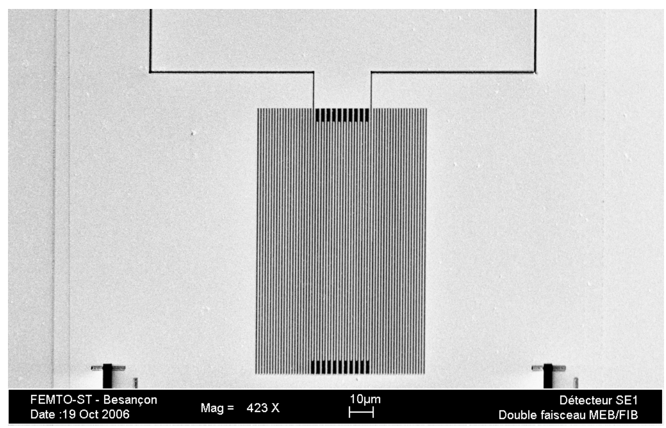

Figure 2. General view and leading dimensions of the first device (aperture 40 µm, length 30 µm)

In fig.4, one can note that the side walls of the strip exhibit a rough surface, due to the etching process. This does not prevent the launching and detection of SAW but may affect the quality of the electrical response of the device and may generate additional losses due to diffusion in the grating. Figure 4 also shows that the actual depth of the strip is larger than 50 nm (the metal thickness). This was necessary to ensure a perfect separation of the active electrode and the reference electrode, allowing for an efficient piezoelectric excitation and detection.

C. Characterization and analysis

The propagation of guided elastic waves on PZT/SrTiO3 compound substrates is intrinsically dispersive since the propagation medium is inhomogeneous. Consequently, one has to take into account the evolution of the phase velocity $V\varphi$ versus the frequency-thickness product relative to the PZT overlay thickness and the IDT mechanical period p which will force the operating frequency as $f=V\varphi/2.p$. Figure 4 shows the dispersion curves derived from the Green's function of the substrate [5].

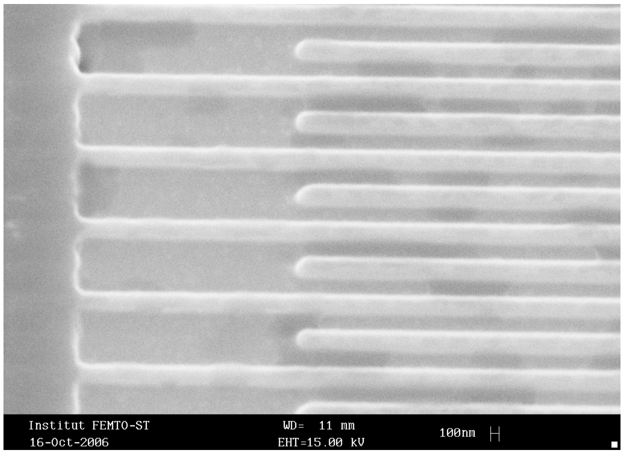

Figure 3. Close view of the transducer's fingers.

The velocity curve (fig.4a) also emphasizes the operating points as the crossing point of the linear law relating the thickness and the IDT period fixed to 0.5 µm (λ_{ac}=1µm) [6]. It appears that the first mode always is weakly coupled, and that doubling the wavelength would considerably increase this figure. However, the second mode should exhibit much larger values of coupling, yielding attractive opportunities for RF wide bandwidth filter applications.

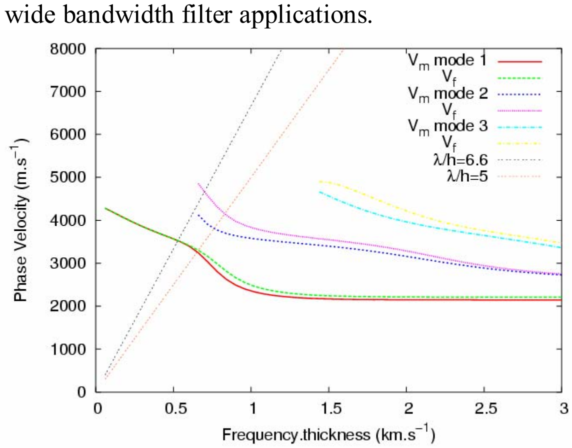

(a)

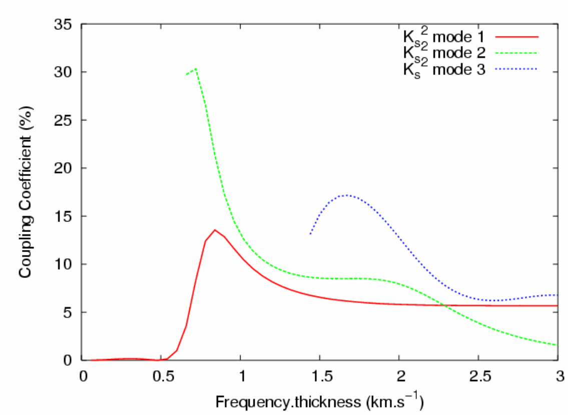

(b)

Figure 4. Dispersion curve of PZT layer deposited on $SrTiO_3$, (a) velocity and (b) coupling coefficient vs frequency-thickness product

To check these theoretical predictions, devices have been tested using a RF tip-probing bench Süss Microtech PM 5 together with a Rohde & Schwarz ZVCE network analyzer, allowing the admittance of the devices to be directly accessed. This parameter can be advantageously compared to harmonic admittance computed using a mixed boundary integral/finite element model dedicated to dispersive substrates [7].

A second set of experiments then was engaged to better understand and to analyze the wave operation on such substrates. PZT layers have been deposited and their thickness has been measured using X-ray size effects and respectively found equal to 150 and 200 nm. Eight devices have been etched and seven have been actually tested. The following graphs show the superimposition of the experimental admittance of the tested devices and the harmonic admittance computed considering the expected shape of the strip. The equivalent thickness of the film has been fit to allow for a good matching, because the theoretical approach only is able to handle flat interfaces. The equivalent thickness is reported in the figure caption, always ranging from 100 to 150 nm. The origin of the discrepancy between the actual film thickness and the value used in the calculations has to be further investigated.

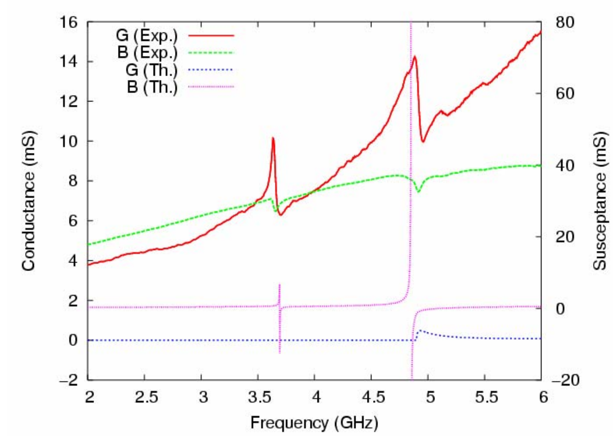

(a)

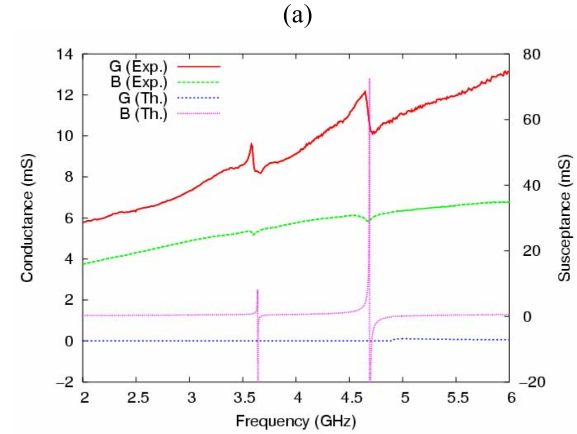

(b)

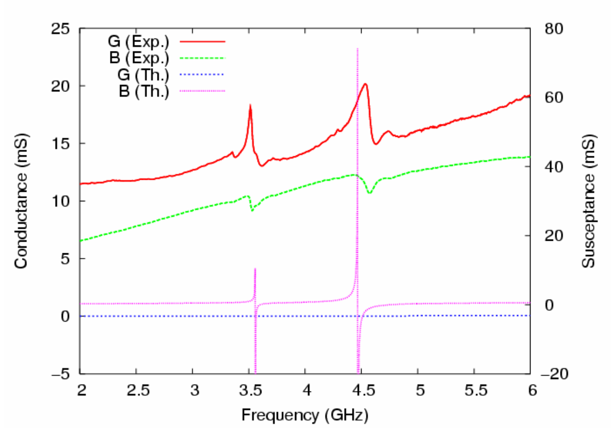

(c)

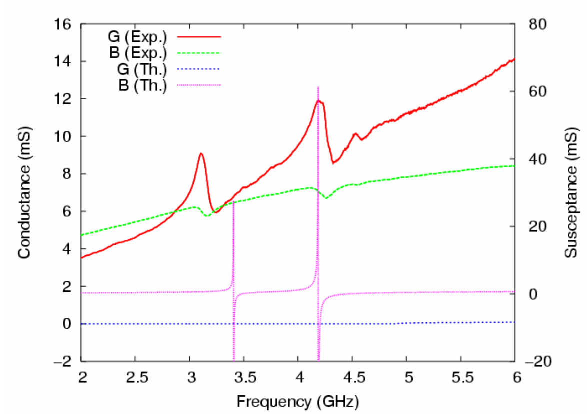

(d)

Figure 5. Electrical responses of the 2nd run devices and comparison with theoretical predictions obtained by fitting the PZT equivalent thickness (a) 100 nm (b) 110 nm (c) 125 nm (d) 150 nm

The approach consisting in fitting the equivalent provides a good agreement between theory and experiments for most of the tested devices but fails in the case of the device corresponding to fig.5d. This should correspond to a 200 nm thick PZT film on which the etching deeply penetrates in the piezoelectric layer. In that case, the acoustic-electrical coupling conditions are quite different from the plane interface situation and requires another kind of analysis as well as more structural characterization. In fig. 5a,b and c, the electromechanical coupling coefficient is found equal to 0.5 and 0.8% for the first and second mode respectively, whereas these values reaches 1.6 and 2.8% for the device of fig.5d. These experimental values are rather far from theoretical values, but the latter was computed using elastic, piezoelectric and dielectric constants of standard bulk PZT (typically PZT-4 material data [8]) which does not correspond to the implemented layer. Consequently, more theoretical work has to be achieved for a more accurate analysis of the experimental results. Nevertheless, one can note that resonance frequencies are correctly predicted (at least the scale order) as well as the general behavior of the devices.

IV. Conclusion

The possibility to implement FIB techniques for the fabrication of high frequency SAW devices on epitaxial PZT layers has been investigated in this work, showing that GHz range prototypes could be successfully manufactured and tested. Resonators operating in the range 3-5 GHz have been fabricated and successfully tested. IDTs exhibiting electric period of 1 µm (acoustic wavelength) have been manufactured to ease measurement interpretation and test the upper frequency limit reachable along this approach. It appears that the technology certainly could be pushed one step ahead, allowing for 500 nm wavelength SAW devices to be manufactured. This is the next target we intend to meet and eventually cross over. Another aspect of this process is its capability to pattern complicated structures, to test actual 3D electrode and strip shapes for investigating new classes of surface devices.

Acknowledgment

This work is supported by the EC in the INTERREG III A framework – France Switzerland – identify as the DOMINOS project. Part of this work was supported by the Swiss National Science Foundation through the National Center of Competence in Research "Materials with Novel Electronic Properties-MaNEP" and Division II, and ESF (Thiox).

References

[1] C.C.W. Ruppel, T.A. Fjeldly, "Advances in Surface Acoustic Wave Technology, Systems & Applications (Vol.1 & 2)", World Scientific Publishing Co. Pte. Ltd., 2000

[2] Knauer, U. Machui, J. Ruppel, C.C.W. , "Design, fabrication, and application of GHz SAW devices", Microwave Symposium Digest 1997, IEEE MTT-S International, Vol.3, pp. 1821-1824

[3] T. Tybell, C. H. Ahn, and J.-M. Triscone, "Control and imaging of ferroelectric domains over large areas with nanometer resolution in atomically smooth epitaxial $Pb(Zr_{0.2}Ti_{0.8})O_3$ thin films" , Appl. Phys. Lett. 72, pp. 1454-1456, 1998

[4] R. Salut, W. Daniau, H. Majjad, S. Ballandras, "Direct writing of high frequency surface acoustic waves using focus ion beam etching", Proc. of the IEEE Ultrasonics Symposium, 2006

[5] A. Reinhardt, T. Pastureaud, S. Ballandras, V. Laude, "Scattering matrix method for modeling acoustic waves in piezoelectric, fluid, and metallic multilayers", J. of Appl. Phys., Vol. 94, n°10, pp. 6923-6931, 2003

[6] S. Ballandras, A. Reinhardt, A. Khelif, M. Wilm, V. Laude, W. Daniau, V. Blondeau-Pâtissier, "Theoretical analysis of damping effects of guided elastic waves at solid/fluid interfaces", Journal of Applied Physics. 2006.99.054907

[7] S.Ballandras, A. Reinhardt, V. Laude, A. Soufyane, S. Camou, W. Daniau, T. Pastureaud, W. Steichen, R. Lardat, M. Solal, P. Ventura, "Simulations of surface acoustic wave devices built on stratified media using a mixed finite element/boundary integral formulation", J. of Appl. Phys., Vol. 96, n°12, pp. 7731-7741, 2004.

[8] Landolt-Börnstein, *Numerical data and functional relationships in science and technology*, Group III, Crystal and solid state physics, Vol. 11, K.H. Hellwege and A.M. Hellwege Eds., Springer-Verlag Berlin – Heidelberg – New York, 1979